

SIXTH FRAMEWORK PROGRAMME



Project contract no. 003933

THRESHOLDS
Thresholds of Environmental Sustainability
INTEGRATED PROJECT

Priority 1.1.6 "Sustainable Development, Global Change and Ecosystems"
Sub-Priority 1.1.6.3 "Global Change and Ecosystems"

Stream 2 – D2.1.2
***Report on effects of the degree of spatial and
 variable's aggregation into threshold behaviour***

Due date of delivery: December 2006
 Actual submission date: January 2007

Start date of project: 1st of January 2005

Duration: 48 months

Lead authors for this deliverable: Emilio Hernández-García (CSIC-IMEDEA)
 Flora S. Bacelar (CSIC-IMEDEA)

Project co-funded by the European Commission within the Sixth Framework Programme (2002-2006)		
Dissemination Level		
PU	Public	X
PP	Restricted to other programme participants (including the Commission Services)	
RE	Restricted to a group specified by the consortium (including the Commission Services)	
CO	Confidential, only for members of the consortium (including the Commission Services)	

Contents

EXECUTIVE SUMMARY	3
1 INTRODUCTION	4
2 THRESHOLDS AND SPATIAL SCALE	7
2.1 AN EUTROPHICATION MODEL AT DIFFERENT SCALES . . .	8
2.1.1 The model and its behavior	8
2.1.2 Observations at different scales	12
2.2 DISPERSION AND SIZE EFFECTS	14
3 AGGREGATING PREYS IN A PREDATOR-PREY MODEL	16
3.1 PREDATOR EXTINCTION THRESHOLDS WITH TWO PREYS	20
3.2 NUMERICAL EVALUATION OF STEADY STATES	22
4 CONCLUSIONS	24

List of Figures

1	Configuration of a predator-prey interacting system	4
2	Prey densities at various scales	5
3	Illustration of food web aggregation	6
4	The recycling function $R(P)$ of Carpenter et al. (1999)	9
5	Spatial configurations from the model in Carpenter et al. (1999) . .	10
6	Spatiotemporal evolution	11
7	Temporal evolution of densities averaged over regions of different size	13
8	Hysteresis loops at several diffusion values for non-stochastic load	14
9	Hysteresis loops at several diffusion values for stochastic load . .	16
10	One consumer of several primary producers	17
11	Steady solutions for one producer and one consumer	19
12	Histogram of predator extinction thresholds	21
13	Time evolutions for $N=2$	23
14	Time evolutions for $N=3$	24
15	Steady state values for $N = 2$	25
16	Steady state values for $N = 3$	26

Executive summary

The values of driver variables at which thresholds and regime shifts occur, and even their presence or detectability, depend on the scale at which natural systems are observed or modelled. In this report we consider by means of particular model examples two kinds of aggregation processes involving description at a larger scale, and observe how threshold phenomena become modified. Spatial aggregation is illustrated within a model of lake eutrophication, and variable aggregation is performed in a model with several competing primary producers. Although it is not easy to extract general conclusions, one of them seems to be that clear thresholds and nonlinear dynamics are less likely to be observed in aggregated descriptions, involving the average of many variables, than in more detailed ones.

1 Introduction

Understanding the effects of the aggregation of variables is one of the fundamental problems in ecological modelling. In fact, deciding which variables to investigate is one of the first steps either in experimental or in theoretical scientific work. This choice in the level of description will necessarily have an impact in the evaluation of thresholds and points of non-return which are the focus of the THRESHOLDS integrated project. The aim of this report is to investigate variations on threshold behavior induced by changes in the aggregation level of the variables studied.

Two conceptually different modes of aggregation are considered here: **spatial aggregation** and **aggregation of variables**. The first one is illustrated in Figs. 1 and 2 (from Pascual and Levin (1999)).

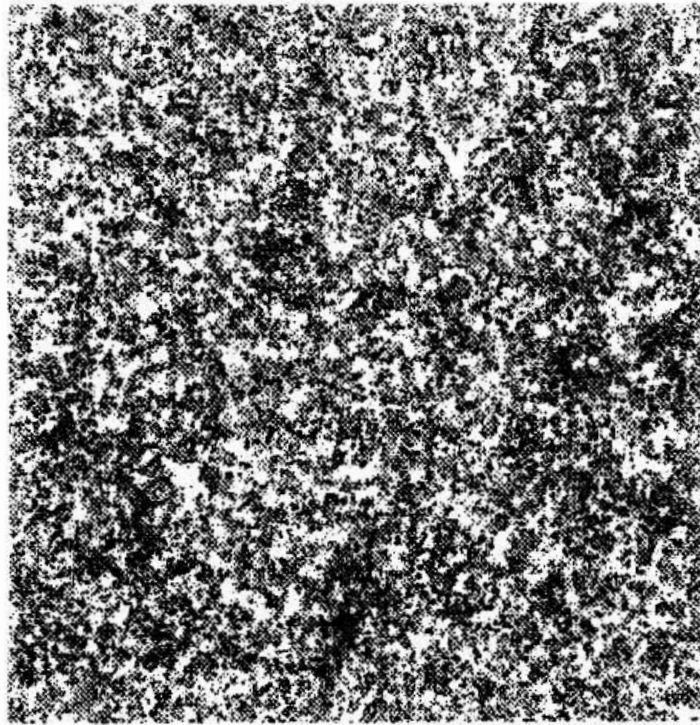


Figure 1: Spatial configuration of a predator-prey system interacting on a square lattice. Black points are predators and white are prey.

Figure 1 shows a snapshot of the configuration of a spatially explicit predator-prey model in which the organisms move in a two-dimensional square lattice (Pascual and Levin, 1999). A common variable to characterize the dynamics is to use a density, i.e. the number of organism in a given area, and then the issue of choos-

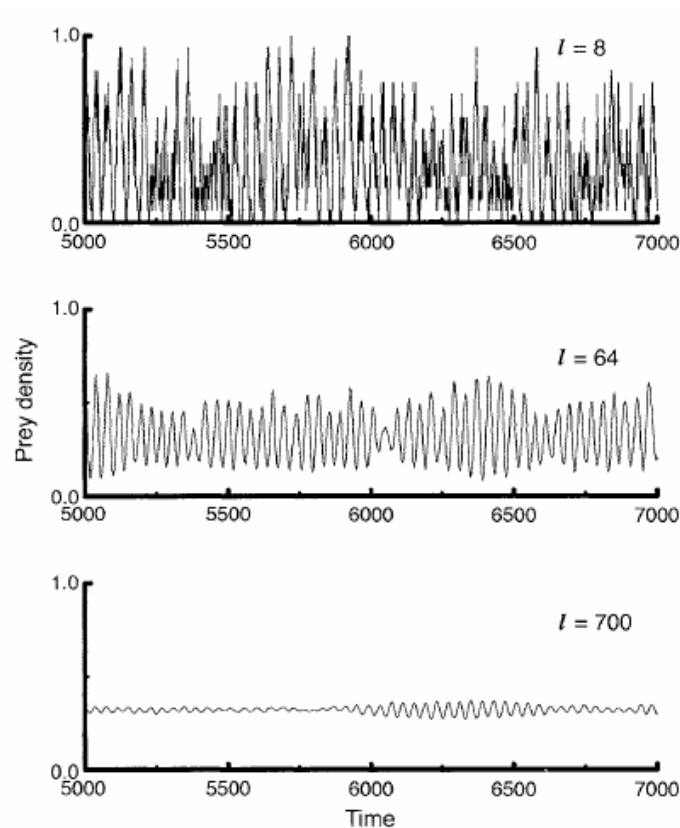


Figure 2: Prey densities from a predator-prey model at different scales (Pascual and Levin, 1999). Top is the density in a particular 8×8 spatial window, middle in a 64×64 window, and bottom in one of size 700×700 (which is the full system size).

ing the relevant elementary area arises. We shall not discuss whether or not a ‘correct’ or ‘optimal’ area size exist, nor the criteria to choose it (see for example Pascual and Levin (1999) or Pascual et al. (2001)), but we will show examples of the different threshold behavior observed when different choices are made. Figure 2 displays the temporal dynamics of the density defined at different scales, a small area in the top plot, the whole system in the bottom one, and an area of intermediate size in the middle one. At small scales dynamics appears quite irregular and intermittent. Noisy but clear oscillations with a well defined frequency are observed at intermediate scales. When increasing further the observation scale oscillation amplitude decreases until being barely observable when the descriptive variable averages information from the whole system (bottom plot).

The second mode of aggregation, ecosystem description by (nonspatially) aggregated variables, is illustrated in Fig. 3. A complex ecosystem may be repre-

sented by the individual taxonomic species (Figure 3, left), or by a much simplified representation such as the one in the right part of the figure, in which nodes represent groups of species sharing approximately the same trophic level and position. Other representations would describe the ecosystem in terms of *trophic species*, i.e. functional groups that contain organisms that appear to eat and be eaten by the exact same species within a food web (Cohen and Briand, 1984). Other examples are the definition of functional groups in communities (Hay, 1994; Steneck and Dethier, 1994), trophic levels in food webs (Armstrong, 1994), and demographic classes in populations (Caswell and Hohn, 1992). It is likely that a simplified representation will miss some of the threshold phenomena which can be present in the detailed one, as the replacement of one species by other pertaining to the same functional group. Also, oscillations and fluctuations will be less evident or even absent in the aggregated description. We note that even the ‘detailed’ food web structure on the left part of Fig. 3 is already a coarse representation of nature, as the data used to build it were collected from 24 different locations (see <http://foodwebs.org/GrassTrophicWebInfo.html>), which are not distinguished in the plot. Also, biological species consists finally in a number of individuals, which are not explicit in any of the representations in Fig. 3.

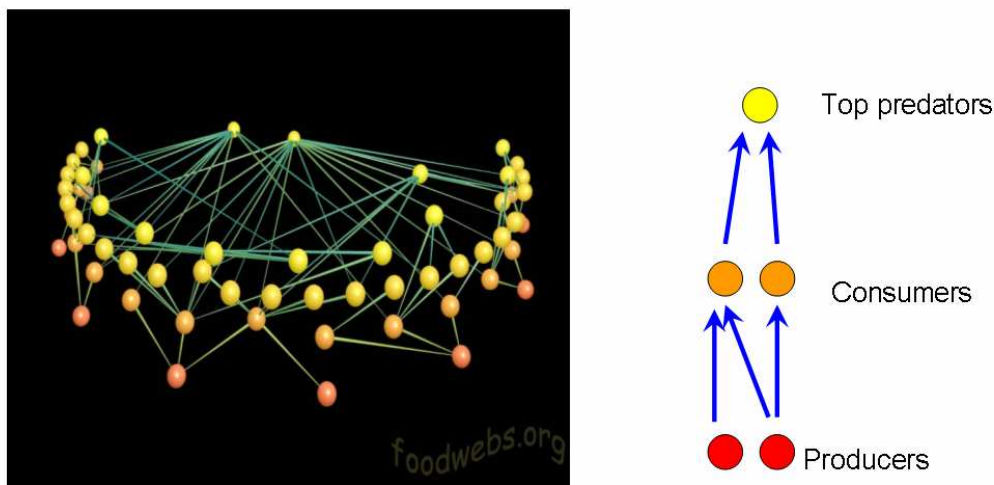


Figure 3: Example of variable aggregation in a food web. Left: UK Grassland foodweb (from <http://foodwebs.org>). Red spheres represent primary producers and detritus, and orange and yellow are consumers and predators. The links represent trophic links. Right: a very simplified representation in which the whole ecosystem description is reduced to two primary producers, two consumers, and one top predator.

The motivation for proposing the present deliverable was the recent development of recent techniques, relatively simple and general, that allowed to map the

bifurcation behavior of large scale variables from the behavior of the individual components (de Monte et al., 2004; Tessone et al., 2006, 2007). The aim was to analyze these techniques and apply them to ecosystem models relevant in the context of the THRESHOLDS Integrated Project. It turned out however that, although of a quite general character, these novel methodologies were devised for dynamical systems with some characteristics that make them quite different from the most relevant to the Integrated Project: on the one hand, global coupling and a high degree of symmetry (i.e. all individuals interact with all the others and in the same way) is assumed, and on the other a kind of *cooperative* coupling is used, which leads to synchronization phenomena. The *antagonistic* interactions more common in ecology (e.g. predator-prey, or parasite-host) do not fit into the above framework. As a consequence the results presented here are of a nature more specific than expected.

We divide the report in two main sections. In Sect. 2 we further motivate the study of spatial effects on threshold behavior, and then illustrate them on the model developed by Carpenter et al. (1999) to manage lake eutrophication. Our interest is not to reach conclusions or prediction on particular aquatic ecosystems, but to show examples of the changes in thresholds that occur when spatial effects are taken into account and how they depend on observation scale (Subsect. 2.1). Subsect. 2.2 discusses the related issue of system size and noise effects. In Sect. 3 we describe a very simple Volterra-type dynamics involving one predator or consumer, and several prey or primary producers. This will provide the framework in which we show examples of changes in threshold behavior when aggregating the prey variables into a single class. We present the analytic estimation of a particular extinction threshold (Subsect. 3.1) and a full numerical simulation of the system fate under different parameter sets (Subsect. 3.2). In the final section we compile our conclusions.

2 Thresholds and spatial scale

Individual based models which follow the fate of each organism in a model ecosystem are becoming increasingly popular, as the individual is both a fundamental ecological unit and also a natural scale for taking measurements. But prediction from this kind of models is hindered by the large amount of parameters they include, and by the difficulty in obtaining results by means other than computer simulations. Therefore most of thresholds and regime change model studies have been done in terms of models that either completely neglect any spatial inhomogeneities of the system considered (the organisms are then considered to be ‘well mixed’) or they consider variables representing spatial averages of individual characteristics in some more or less small region. The large span of scales

between the individual level and the size of a large ecosystem makes the problem of spatial pattern and scale one of the fundamental issues in ecological thinking (Levin, 1992).

Strongly associated with questions on spatial scale, there are at least two other important phenomena: noise and transport. Individual based systems are usually of stochastic type, reflecting the fundamental unpredictability of the detailed behavior of individual organism. When describing the system in terms of spatial averages most of the stochastic fluctuations get smoothed (see for example Fig. 2), but they never disappear completely and, more importantly, their presence at the small scales may have a qualitative impact even on averaged macroscopic variables (Pascual et al., 2001). Thus, noise effects should be taken into account when discussing the spatial scaling behavior of thresholds (Guttal and Jayaprakash, 2006). The origin of noise may not be restricted to demographic fluctuations at the microscale: climatic and other environmental fluctuations are always present in any ecosystem. This leads to parameter inhomogeneity and variability, which can also be modelled as adequate noise terms in the governing equations.

On the other hand, the fact that real ecosystems are usually spatially inhomogeneous implies the relevance of transport processes among the different regions of the system. Many ecosystems consist of patches of habitats and some keystone organisms (the mobile link organism, see Gilbert (1980) or Lundberg and Moberg (2003)) actively move between them. Random motion of individuals can be modelled as a diffusion process at larger scales. This is but another example of a microscopic noisy process –individual random walks– producing a deterministic and important effect at large scales: the smoothing processes of macroscopic densities which is called diffusion. Other types of individual dispersal (e.g. Lévy flights) lead to different macroscopic behavior (e.g. superdiffusion, Viswanathan et al. (1996), Nathan et al. (2002)). In addition to diffusion and diffusion-type dispersal, fluid flow is a transport processes which strongly influences biological dynamics (Hernández-García et al., 2003; Peters and Marrasé, 2000).

2.1 An eutrophication model at different scales

2.1.1 The model and its behavior

In order to illustrate the joint effect of spatial extension, transport and noise at diverse scales, we consider the following extension of the model by Carpenter et al. (1999) describing phosphorous cycling in stratified lakes:

$$\frac{\partial P}{\partial t} = F - sP + r \frac{P^q}{K^q + P^q} + D \frac{\partial^2 P}{\partial x^2} \quad (1)$$

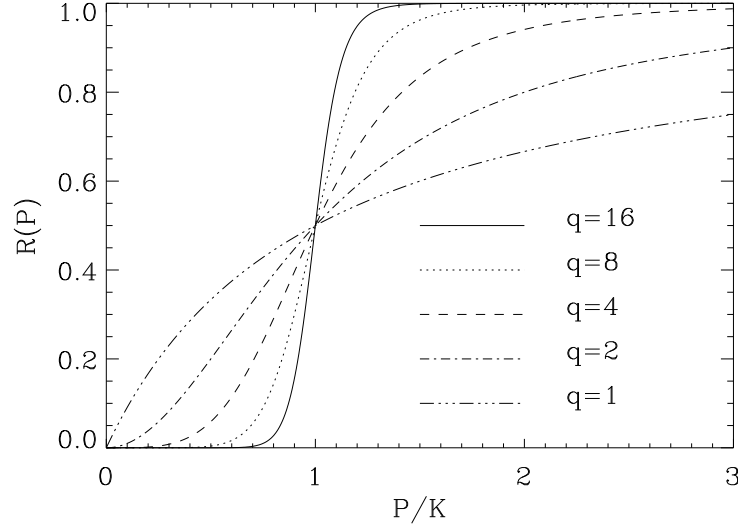


Figure 4: The recycling function $R(P)$ (Eq. (2)) of Carpenter et al. (1999) for several values of the exponent q . For large q there is a large increase of phosphorous recycling towards the water column when $P \gtrsim K$.

$P = P(x, t)$ is the phosphorous density in the water column at time t and location x of a one-dimensional aquatic system (extending from $x = 0$ to $x = L$). F is the rate of phosphorous input into the system (nutrient load), s is the inverse time scale describing the rate at which phosphorous is removed from the water column, both by escape from the aquatic system and by incorporation into the sediments. The third term contains the function

$$R(P) = \frac{P^q}{K^q + P^q}, \quad (2)$$

which is displayed in Fig. 4. It models the recycling of phosphorous from the sediments back into the water. There is a sharp increase of this recycling when the ambient concentration exceeds a particular value K , related to the phosphorous concentration at which the aquatic system becomes anoxic. The exponent q controls how steep this increase is. r sets the maximum amount of recycling. Finally, there is diffusive transport of phosphorous along the spatial extent of the system, characterized by the effective diffusion coefficient D . The model by Carpenter et al. (1999) has been studied by many authors, since it is a classical example of a simple mechanism dealing to bistable behavior and regime shift: for small nutrient load F , the system is in a low phosphorous (oligotrophic) state, which could be approximated by $P \approx F/s$, but a sharp transition to an eutrophic state

occurs when F is increased, a change that may be difficult or even impossible to reverse when decreasing F again: the model presents hysteresis effects. At large F the eutrophic state can be approximated by $P \approx (F + r)/s$. The main variable in the model, the phosphorous concentration $P(x, t)$, not a biotic, but a chemical quantity. Nevertheless, since the dynamics described by the model, lake eutrophication, clearly involves biological mechanisms, we will refer to the system described by Eq. (1) as an *ecosystem*.

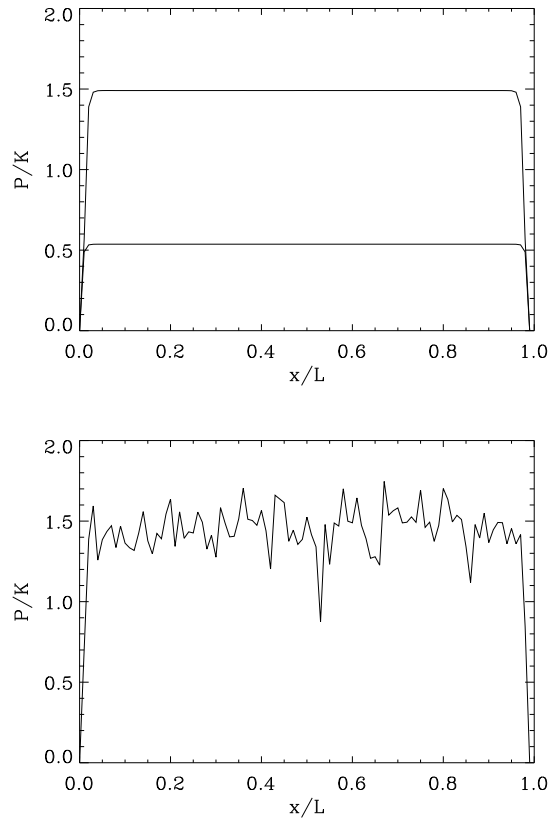


Figure 5: Spatial configurations from Eqs. (1) for parameters $q = 8$, $r = 1$, and $D = 10^{-5}$ (without loss of generality, we can choose $L = s = K = 1$). Top: $F = 0.53$ and no noise. The two stable configurations are shown. Bottom: stochastic load, $F = \bar{F} + \xi(x, t)$, with mean $\bar{F} = 0.53$, and ξ a Gaussian white noise of zero mean and correlations $\langle \xi(x, t)\xi(x', t') \rangle = \kappa^2\delta(x - x')\delta(t - t')$, with noise intensity $\kappa = 1.6$.

A spatially extended version such as the one in (1), which contains the diffusive term, has been considered by van Nes and Scheffer (2005). A simple rescaling analysis of Eq. (1) shows that increasing the diffusion coefficient D by a factor f has the same effect as reducing system size L by a factor $f^{1/2}$. The influence of

noise has been also recently addressed (Guttal and Jayaprakash, 2006). Although many sources of noise and variability may be present in lakes such as the ones for which Eq. (1) was devised, we consider here fluctuations in the nutrient load parameter F . It is expected that larger aquatic systems receiving input from larger basins will experience a less intermittent input than smaller ones and, in this sense, changing the noise intensity is also a way of probing size and scale.

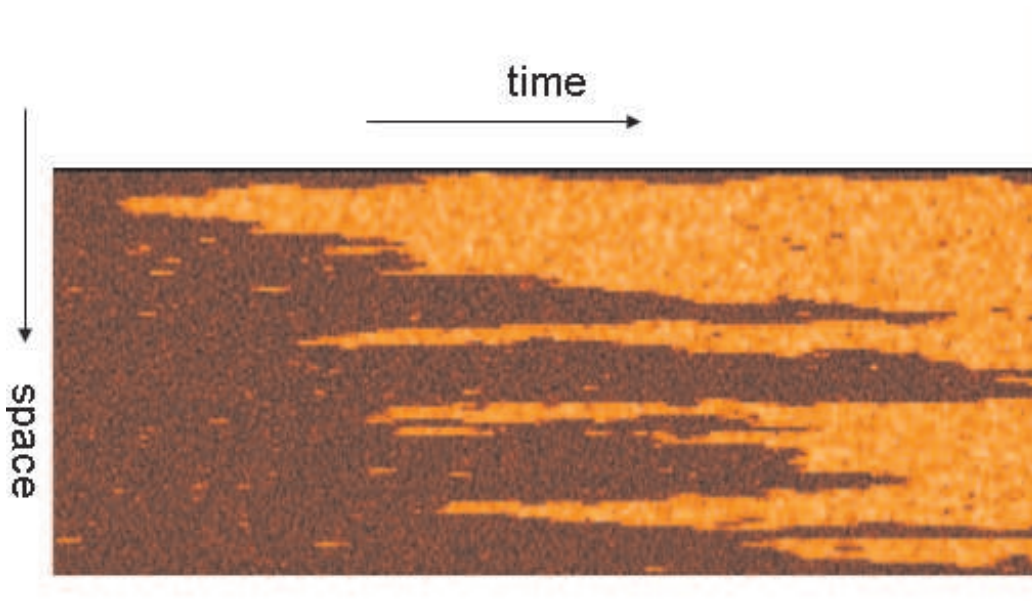


Figure 6: Spatiotemporal representation of the evolution of system (1) under stochastic load, obtained by computer simulation. Phosphorous concentration is coded by color shades, with clearer tones corresponding to higher values. The initial condition is close to the oligotrophic state (dark red). Parameter values are as in Fig. 5 (bottom), for which the fluctuating evolution tends to approach the proximities of the eutrophic state (light orange). The existence of two preferred alternative states is clearly observed. Domains close to the eutrophic one are nucleated and progressively spread, until filling the full system at long times (total displayed simulation time 600 time units (in units of s^{-1})).

Figure 5 (top) shows the two spatial configurations that can be attained, depending on initial conditions, by the solution of the model (1) at long times for constant input $F = 0.53$. We have taken s , K , and L as the units of time, phosphorous concentrations, and space, so that without loss of generality $s = K = L = 1$. The other parameter values are $q = 8$, $r = 1$, and $D = 10^{-5}$. The boundary conditions used are $P = 0$ at $x = 0$ and $x = L$. This corresponds to a system receiving input all along its spatial extent, and diffusively releasing phosphorous from the two extremes. This is not a very realistic configuration for a lake but it is certainly

more adequate than the periodic boundary conditions usually used in theoretical studies. There are boundary layers of size proportional to $D^{1/2}$ close to each end of the system. Outside of them phosphorous is constant, but there are two possible values of this constant at these parameter values chosen, a consequence of the dynamic bistability characteristic of the model.

We now discuss the case of stochastic nutrient load. We take it to be $F = \bar{F} + \xi(x, t)$, where F is a mean input, and $\xi(x, t)$ is a Gaussian white noise of zero mean and correlations given by $\langle \xi(x, t) \xi(x', t') \rangle = \kappa^2 \delta(x - x') \delta(t - t')$. Now, $P(x, t)$ does not reach a steady state, but it is continuously fluctuating in response to the stochastic input. Figure 5 (bottom) shows a representative instantaneous configuration in such state for the same parameter values as before, but with stochastic load of mean $\bar{F} = 0.53$ and noise intensity $\kappa = 1.6$. Although changing and inhomogeneous, phosphorous concentrations remain close to the eutrophic state nearly everywhere during most of the time. This high concentration is more resilient to noise than the oligotrophic one at these parameter values.

If starting with an initial condition close to the oligotrophic state, fluctuations will drive a change of regime towards the eutrophic state. This is illustrated in Fig. 6. After some initial waiting time, fluctuations create small areas occupied by the eutrophic state which, because of its higher relative stability (Guttal and Jayaprakash, 2006), spread into the system gradually replacing the oligotrophic regions. Finally the whole system is in a noisy eutrophic state close to one existing in the absence of noise. We emphasize that in the absence of noise (see Fig. 5, top) or without spatial dependence the system is strongly bistable for these parameter values. Noise is acting to decrease the width of the hysteresis loops. This will be seen more clearly in Subsect. 2.2.

2.1.2 Observations at different scales

The whole process seen in Fig. 6 can be understood as an initial clear water state, established perhaps after a long period of stable low mean values of nutrient load, and a change of regime occurring after the mean load has risen to a higher level. The transition between the initial and the final state can be observed at different spatial resolutions. To compare the diverse outcomes is one of the main motivations for the present report. We illustrate them in Fig. 7. The top panel shows phosphorous concentration averaged in a small spatial interval (which corresponds to a single lattice site in the computer simulation). The middle one shows the average concentration in a region about six times larger, and finally the mean concentration averaged over the whole system is shown in the bottom panel. The top panel confirms what is seen in the spatiotemporal representation of Fig. 6: that the regime shift is rather sharp at any spatial point in the system. The particular time at which the regime jump occurs is different at different spatial locations, but

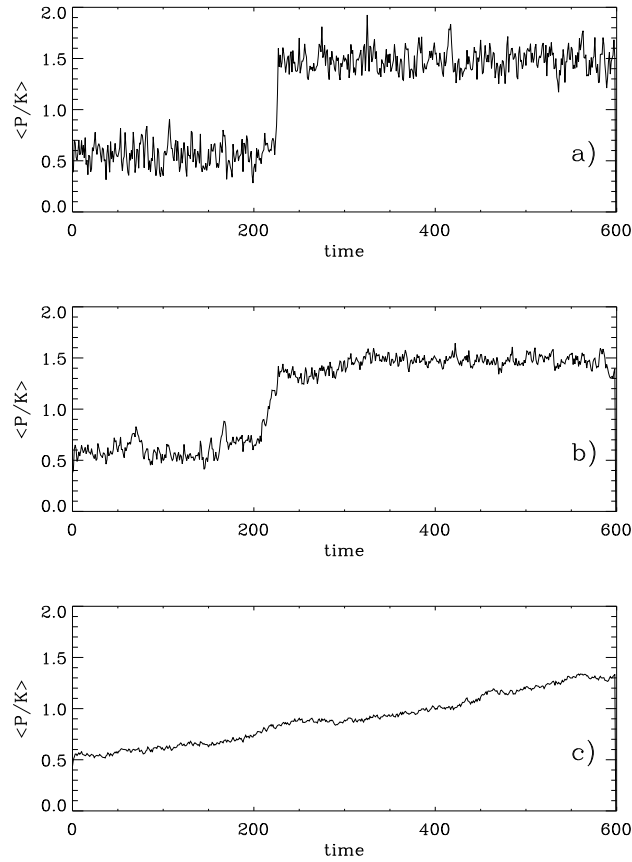


Figure 7: Time evolution of phosphorous densities averaged in regions of different sizes (lengths in units of system size $L = 1$) from the simulation in Figure 6: a) Density averaged in the small interval $[0.23, 0.24]$, b) in the larger interval $[0.20, 0.26]$, c) density averaged over the whole system $[0, 1]$.

all of them display a similar behavior. The discontinuous transition is however blurred when averaging the density at larger scales. Finally, only a smooth growth is seen when considering the average over the whole system.

The pattern described above is consistent with what is seen in the different system displayed in Fig. 2, but there a second side effect of spatial averaging is of importance: We observe in both Fig. 7 and Fig. 2 that fluctuations occurring on top of the main dynamic feature in these time evolutions (a single jump in Fig. 7 and oscillatory behavior in Fig. 2) become also smaller when averaging at larger sizes. This is the classical effect of averaging: it decreases noise. This has as a consequence that the dynamic behavior of the spatial predator-prey model of Fig. 2 is clearer in the middle panel than in any of the other observation scales.

Averaging diffuses away the dynamic behavior but also cleans up the fluctuations on top of it. Which of these effects is stronger, determining which spatial scale of observation is more adequate to determine clean thresholds, would depend on the particular system under consideration.

2.2 Dispersion and size effects

As indicated above, increasing the intensity of spatial dispersion, parameterized in the diffusion coefficient D , is equivalent to reducing system size. Thus, exploration of the effects of changing D is also a way of probing size and scale effects in the model.

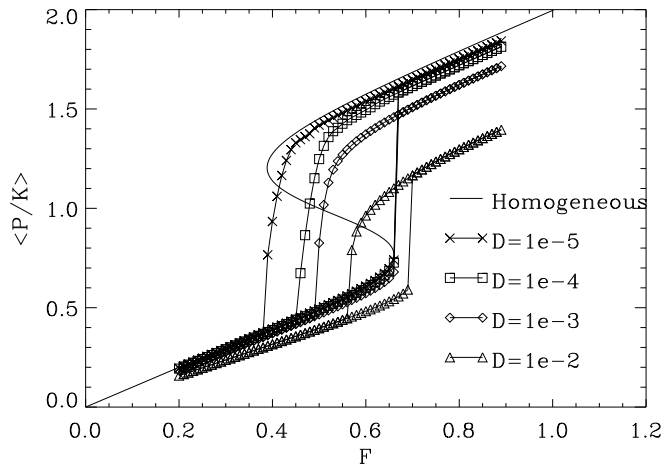


Figure 8: Phosphorous concentration averaged over the whole system, for diffusion coefficients $D = 10^{-5}, 10^{-4}, 10^{-3}, 10^{-2}$ and in the absence of nutrient load noise. Hysteresis loops are followed by first slowly increasing and then slowly decreasing F . At each value of F the system response is let to equilibrate for 30 time units (units are s^{-1}) before recording the corresponding concentration average. The rest of the parameters as in Fig. 5. Solid line gives the steady solutions of Eq. (1) in the absence of spatial dependence.

Figure 8 shows the phosphorous concentration averaged over the whole system, obtained from computer simulation for several values of D , as a function of the nutrient load F (which is kept constant for 30 time units to obtain each simulation point). Solid line is the analytic steady state of Eq. (1) when the whole system is assumed to be homogeneous (and thus the diffusion term is not present).

Bistability and hysteresis persist for all values of D , but there are quantitative changes. For increasing diffusion the range of bistability and the jump size decrease. The decrease in the concentration values corresponding to the eutrophic

state for large diffusion are particularly noticeable. A related observation is that the hysteresis loop of the homogeneous system is approached when D decreases. This is in contrast with many studies in which homogeneity is approached in the opposite limit, that of very large diffusion $D \rightarrow \infty$. The explanation is in the boundary conditions we use in the presence of diffusion: since we force $P = 0$ at the system ends, corresponding to diffusive escape of concentration, increasing diffusion increases the escape and the homogenization in this case dilutes away all the phosphorous. Thus, the $D \rightarrow \infty$ leads in this case to $P = 0$ everywhere. The tendency to lower values of P for larger D is seen in Fig. 8 for the curves of largest D . In our case, the limit of a homogeneous but non-vanishing concentration is approximated rather when $D \rightarrow 0$ because, when the system is large (equivalent to small D), most of its extent has concentration values determined by the internal nonlinear dynamics and independent of the boundary conditions. The effect of the boundaries just creates boundary layers at the system extremes in which concentration rapidly decreases to zero (see Fig. 5). These layers become smaller for smaller D and become unimportant when calculating system average quantities when $D \rightarrow 0$. This particular outcome is a consequence of the particular boundary conditions used. Other prescriptions may lead to a different behavior, but the message here is that size (or dispersion) matters, and that the predictions obtained from models which do not take into account the spatial extent of an ecosystem nor their spatial inhomogeneities would only apply in some special limit.

An analogous study but for the case of fluctuating F is displayed in Fig. 9. Here the mean value of the load, \bar{F} , is ramped to trace the hysteresis loops. Now the system does not settle in a steady state, but continuously fluctuates. Since, at variance with the related study by Guttal and Jayaprakash (2006), our noise term is unbounded, system state may explore virtually arbitrary configurations at sufficiently long times. Thus, one should specify further how to characterize the ensemble of visited configurations. The temporal mean of the spatial configuration will be a sensible choice. But for most of the parameter values, and during the time scale of our simulation, we do not observe particularly strong jumps between states, being configurations (after waiting the 30 time units we let the system equilibrate each time \bar{F} is increased or decreased) nearly always of the type shown in Fig. 5 (bottom), well characterized by its spatial average at a fixed point. The exceptions are the configurations precisely at the ends of the hysteresis loops (as is the case with the simulation in Fig. 6), where dynamics becomes slower and more time is needed to reach the final fluctuating state. Even in these case we prefer to display in Fig. 9 the spatially averaged concentration exactly 30 time units after changing \bar{F} , instead of some time average, since we believe that the former represents better what would be measured in natural systems, where taking averages over times much longer than typical system scales is rarely feasible.

The only consequence of this (we neglect deeper statistical mechanics considerations (Sethna, 2006)) is that sharp but not discontinuous jumps between states signal the limits of the hysteresis loops. We see that the main effects of D on the global behavior are the same as in the absence of noise. The most visible difference, more noticeable at small D , is the reduction of the width of the hysteresis loops. This is a common effect of noise also observed under other setups (Guttal and Jayaprakash, 2006), and was commented already at the end of the previous subsection.

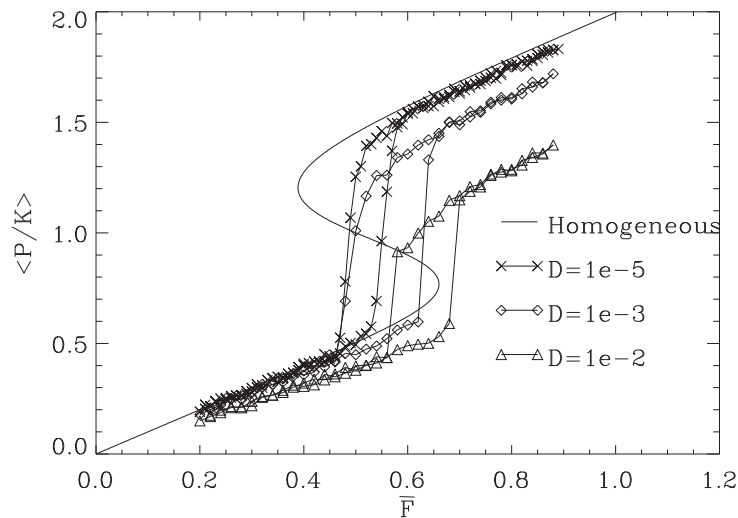


Figure 9: Same as Fig. 8, but with stochastic load: F fluctuates following a Gaussian white noise process of mean \bar{F} , which is varied to obtain the hysteresis loops, and fixed noise intensity $\kappa = 1.6$.

3 Aggregating preys in a predator-prey model

The second type of threshold changes under aggregation we discuss in this report is the one arising in the description of a set of variables by a collective measure. This appears in any attempt to simplify the description of a complex ecosystem, as for example by grouping taxons onto trophic species (Cohen and Briand, 1984), on functional groups (Hay, 1994; Steneck and Dethier, 1994), trophic levels (Armstrong, 1994), or demographic classes (Caswell and Hohn, 1992). In a different context, the conversion of cell cycles into population cycles is a nontrivial process which also arises when describing large ensembles of cells by its total biomass (Pascual and Caswell, 1997).



Figure 10: One consumer of several primary producers and its simplification in terms of two steps of a linear food chain

The structure of a real food web such as the one in Fig. 3 is very complex. But one of the motifs that is repeated several times on it is that of a predator feeding on several preys. Thus, as a basic model with which we can exemplify threshold behavior under variable grouping we can consider one species feeding on a number N of different preys (Fig. 10, left). We close this small subsystem by assuming that the base species are primary producers, feeding on the same resources, and that the predator is a top one only subjected to linear mortality. Thus the primary producers interact competitively because of their coupling by the common resources, and also because of the negative feedback produced by the common consumer on all the producers when one of them grows. As the simplest model describing this situation we have the following Volterra-type set of $N + 1$ equations:

$$\begin{aligned} \frac{dx_i}{dt} &= r_i x_i \left(1 - \sum_{j=1}^N \frac{x_j}{K_{ij}} \right) - g_i x_i Z, \quad i = 1, \dots, N \\ \frac{dZ}{dt} &= Z \left(\sum_{i=1}^N e_i g_i x_i - d \right) \end{aligned} \quad (3)$$

x_1, x_2, \dots, x_N denote the biomasses of the primary producers and Z that of the common consumer. $\{r_i, g_i, e_i\}$ are specific growth rates, predation factors and efficiencies, respectively, and K_{ij} is a competition matrix describing the interactions between producers. The diagonal elements K_{ii} are the carrying capacities, i.e., the biomasses x_i that would be supported by the environment in the absence of the

other producers and of the consumer. The type of interactions among species, bilinear, is very simple and does not include any density dependence, saturation, or similar effects. This choice, commonly taken in studies of this kind (May, 1972, 1973; Thingstad and Sakshaug, 1990; Chen and Cohen, 2001), greatly simplifies analysis, and allows some analytic results to be obtained. It is however a strong simplification, and it is known that even small changes in the interaction functional form may have an impact on ecosystem stability (Gross et al., 2004). Thus, the results we will show should be taken just as an example of threshold behavior under aggregation, and not as generic properties of interacting ecosystems.

If there is only one prey species, the system (3) reduces to

$$\begin{aligned}\frac{dx}{dt} &= rx \left(1 - \frac{x}{K}\right) - gxZ \\ \frac{dZ}{dt} &= Z(egx - d)\end{aligned}\quad (4)$$

There are three steady solutions, which are easy to obtain: a) $x = 0, Z = 0$ is always linearly unstable if $r > 0$. b) $Z = 0, x = K$, the solution in which the consumer is absent, is linearly stable for large consumer mortality: $d > egK$. c) The solution in which the two species coexist:

$$x = \frac{d}{eg}, \quad Z = \frac{r}{g} \left(1 - \frac{d}{egK}\right), \quad (5)$$

becomes positive and stable for smaller consumer mortality $d < egK$. The stable steady solutions are depicted in Fig. 11 as a function of consumer mortality. This system presents a threshold value for the predator mortality, $d_T = egK$, above which the predator becomes extinct. From the mathematical point of view, this threshold arises as a transcritical bifurcation (in the terminology established in the deliverable 2.1.1). We can analyze how this extinction threshold changes when more primary producers are present in the system. The simplest case occurs when all producers are equal:

$$\begin{aligned}\frac{dx_i}{dt} &= rx_i \left(1 - \sum_{j=1}^N \frac{x_j}{K}\right) - gx_i Z, \quad i = 1, \dots, N \\ \frac{dZ}{dt} &= Z \left(\sum_{i=1}^N egx_i - d\right).\end{aligned}\quad (6)$$

Here, closed equation for Z and $X = \sum_{i=1}^N x_i$, the aggregate variable giving the total biomass of all producers are trivially obtained and identical to Eqs. (4), with the individual biomass x replaced by the total one X . Steady solutions are

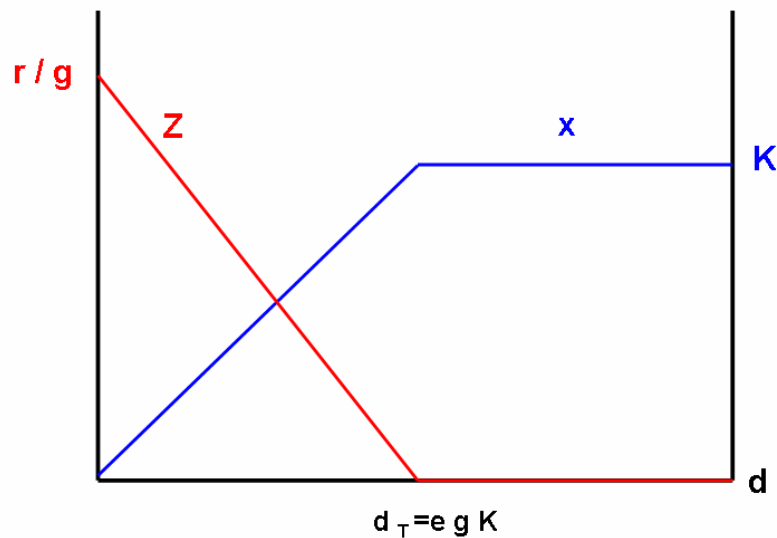


Figure 11: Biomass values at the stable fixed points of the model with one consumer (Z) and one primary producer (x) as a function of consumer mortality d . The consumer becomes extinct at a mortality threshold $d_T = egK$.

thus also given by (5) under the same replacement and the threshold d_T remains unchanged.

If there are differences among the producers, then the situation becomes more complex:

- First, the number of steady solutions rapidly increases: there are $2^{N+1} - 1$ of them in the system with N producers. Thus, there are 3 fixed points when there is one producer, 7 when there are two, 15 when there are three, etc. The different solutions correspond to having all the species extinct, all extinct except x_i , with $i = 1, \dots, N$, then all extinct except two of the producers or the consumer, ..., and so on until having the solution in which all the species have a non-vanishing biomass. This last one, called the ‘interior’ solution is the most interesting one for a system with N producers since all the others are already available in the system with less than N producers or with no predator.
- Second, it is no longer possible to write a closed equation for the set of two variables Z and X , but the dynamics remains dependent on the individual biomasses x_i . This means that trying to describe the system in terms just of the aggregated variable X will lead to some indetermination, and that there will be an increasingly large number of possible steady states (X, Z) for

increasing N (although many of them will not be stable), corresponding to the $2^N - 1$ different possible values of x_1, x_2, \dots, x_N, Z .

- Third, for larger N there is also a larger number of model parameters. Labelling this large set by just a small number of statistical descriptors (for example the means of the growth rates $\bar{r} = \sum_i r_i/N$, of the efficiencies $\bar{e} = \sum_i e_i/N$, etc.) introduces a severe loss of information.

Thus, one can try to describe the behavior of aggregated variables as a function of average parameters, but all the information discarded in this reduced description will show up as stochasticity and noise in the functional relationships found. Whether or not this noise will be large enough to make the description useless is a question that can only be answered in particular cases. In our particular example we will illustrate these effects by calculating the predator extinction threshold dispersion in the case of two preys, and by evaluating the aggregated biomasses in steady state.

3.1 Predator extinction thresholds with two preys

In the case of two producers and one consumer ($N = 2$) a convenient way to parameterize system (3) is as follows: a) We choose the mean growth rate as giving the unit of time, so that, without loss of generality, $r_1 = 1 + \alpha$, $r_2 = 1 - \alpha$. b) We measure the producers biomasses x_1 and x_2 in units of their respective carrying capacities. Thus, in these units, $K_{11} = K_{22} = 1$. c) Finally, we choose Z units so that $g_1 = 1 + \beta$ and $g_2 = 1 - \beta$. We also write $e_1 g_1 \equiv g(1 + \gamma)$ and $e_2 g_2 \equiv g(1 - \gamma)$. After these elections, system (3) can be written as

$$\begin{aligned} \frac{dx_1}{dt} &= x_1 (1 + \alpha - (1 + \beta)Z - x_1 - (1 + \epsilon_1)x_2) \\ \frac{dx_2}{dt} &= x_2 (1 - \alpha - (1 - \beta)Z - x_2 - (1 + \epsilon_2)x_1) \\ \frac{dZ}{dt} &= Z (-d + g(1 + \gamma)x_1 + g(1 - \gamma)x_2) \end{aligned} \quad (7)$$

In this notation, the average parameters $(A_1 + B_2)/2$, with $A_i = r_i, K_{ii}, g_i$, are 1, and the average of $e_i g_i$ is g . The case of identical prey, so that they are in fact a single species, corresponds to $\alpha = \beta = \gamma = \epsilon_1 = \epsilon_2 = 0$, being g and the predator mortality d the remaining free parameters. The steady stable biomasses for Z and the aggregated prey X are, in this case, $X = d/g$, $Z = 1 - d/g$ if the mortality d is smaller than $d_T = g$, and $Z = 0$, $X = 1$ otherwise.

For nonidentical preys, there are seven steady state solutions which experience diverse bifurcations so that the exact threshold d_T at which predator disappear

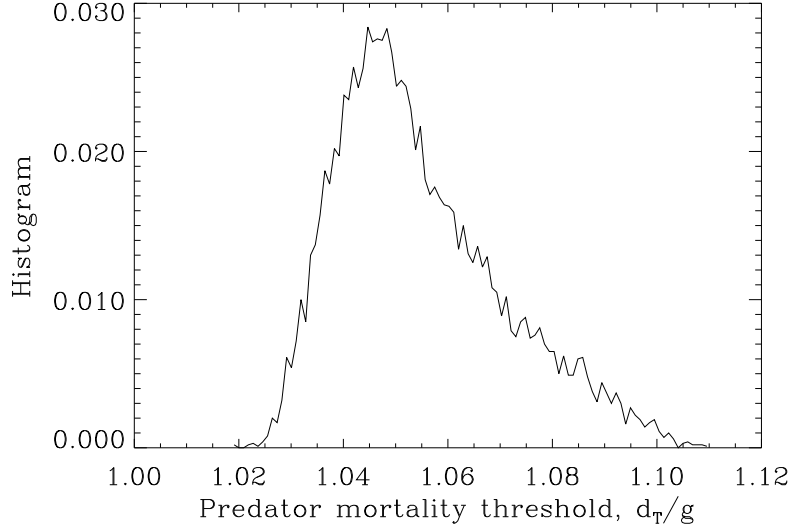


Figure 12: Histogram of predator extinction thresholds. It has been obtained by evaluating Eq. (9) for 10^4 small random values of the parameters $(\alpha, \beta, \gamma, \epsilon_1, \epsilon_2)$. The first three have been drawn from a uniform distribution in $[0.00, 0.05]$, and the last two from a uniform distribution in $[-0.10, -0.05]$.

depends in a complicated way on the stability of the different solutions and on the particular values of all the remaining parameters. As a possible representative value of such threshold, we can calculate the value of d at which the ‘interior’ solution ceases to be positive. This can be done by calculating the biomasses corresponding to that solution, which for the predator reads

$$Z = \frac{d(\epsilon_1 + \epsilon_2 + \epsilon_1\epsilon_2) + g((\alpha + 1)\epsilon_2(\gamma - 1) + 4\alpha\gamma + (\alpha - 1)\epsilon_1(\gamma + 1))}{g((\beta + 1)\epsilon_2(\gamma - 1) + 4\beta\gamma + (\beta - 1)\epsilon_1(\gamma + 1))}, \quad (8)$$

and finding the value of d , d_T , above which Z becomes negative:

$$\frac{d_T}{g} = \frac{-4\alpha\gamma + (1 - \alpha)(1 + \gamma)\epsilon_1 + (1 + \alpha)(1 - \gamma)\epsilon_2}{\epsilon_1 + \epsilon_2 + \epsilon_1\epsilon_2} \quad (9)$$

Since the only parameters remaining in the case of one prey, or in the case in which all preys are identical, are d and g , the right hand side of the above expression represents the variability in the extinction threshold arising from producer differences that keep the average parameters constant. We show in Fig. 12 an example of the impact of this variability. An histogram of values of d_T/g has been collected by evaluating the expression (9) for 10000 small random values of

the parameters. Without loss of generality, only positive values need to be drawn for α , β and γ . For the competition parameters ϵ_1, ϵ_2 we sample negative values in order to favor coexistence of the competing preys (intraspecific competition coefficients $K_{ii}^{-1} = 1$ larger than the interspecific ones $1 + \epsilon_{1,2}$).

We see that there is a dispersion in the value of the thresholds obtained. More important, the distribution is not centered in the value ($d_T/g = 1$) that would correspond to the description in terms of the aggregated variable X with the average value of the parameters. Both effects, however, are small, as corresponding to the rather small differences between the two preys used to generate the histogram in Fig. 12. But we should remind that the calculated mortality threshold refers to just one of the system solutions, not necessarily the one giving the true predator extinction threshold. The stability of the ‘interior’ and ‘noninterior’ (the ones on which some of the prey species is absent) steady solutions needs to be evaluated to fully describe the threshold behavior in our model. We discuss this in the next section, and show that, certainly, the effects of the additional species are much more important than the ones found in this section which has considered just one of the particular solutions.

3.2 Numerical evaluation of steady states

In the previous section we calculated analytically the mortality above which the steady solution of system (3) in which all species are present (the ‘interior solution’) is no longer positive. It may happen that other solutions are stable at these mortality values, and then become relevant to determine the threshold. As a global way to describe system behavior, we perform computer simulations of (3) for randomly generated parameter sets sample values of $\{r_i\}$ and of the non-diagonal entries of $\{K_{ij}\}$ from uniform distributions with mean value 1 and range 5×10^{-3} . The diagonal entries $\{K_{ii}\}$ are fixed to 1, so that the expected values of $\sum_i r_i/N \equiv \bar{r}$ and of $\sum_{ij} K_{ij}/N^2 \equiv \bar{K}$ are both unity (this can be fixed by choice of the units of time and biomass without loss of generality). Mean values \bar{g} and \bar{e} are randomly chosen in $[0, 1]$ and $[0, 0.5]$, respectively, and then values of $\{g_i\}$, $\{e_i\}$ are generated from uniform distributions with these means and range 5×10^{-3} . One value of d is also randomly generated in $[0, 1]$ to complete each parameter set. Initial conditions for all the variables are randomly assigned in $[0, 1]$.

Figure 13 shows, for $N = 2$, examples of the time evolution of the consumer biomass Z and of the aggregated producer biomass $X = x_1 + x_2$ for different parameter sets, showing a great variety of final steady outcomes. Figure 14 shows $Z = Z(t)$ for $N = 3$. We now collect the final constant values of Z and X obtained from each parameter set (we generated 500 of them) and plot them in terms of the average parameters \bar{g} and \bar{e} ($\bar{r} = \bar{K} = 1$) and of d (Figs. 15 and 16).

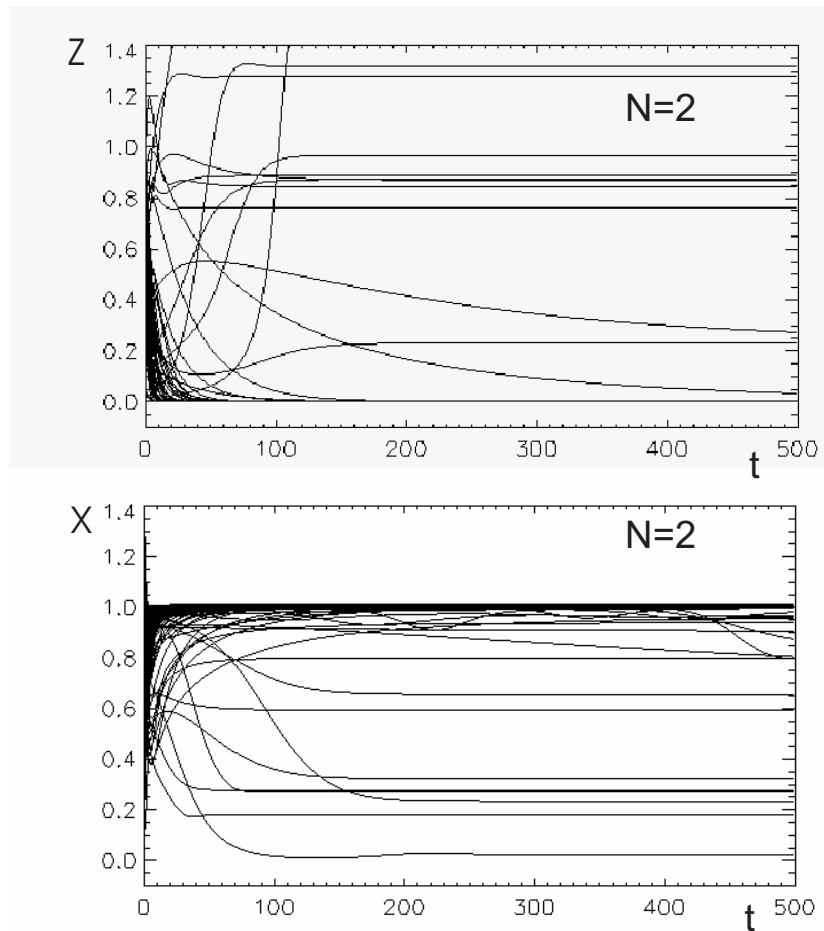


Figure 13: Time evolutions of consumer (Z) and the aggregated producer biomasses (X) from model (3) with $N = 2$ for several randomly drawn parameter sets.

Despite the small variability of the prey parameters around their mean values, a considerable dispersion of the outcomes occurs around the values obtained when preys are identical (solid line). More importantly, simulations for many parameter sets, including some with relatively small consumer mortality, end up in a state with $Z = 0$ and $\bar{q}X/\bar{r} = 1$, both for $N = 2$ and $N = 3$. This means that the presence of several coexisting prey species destabilizes the predator and facilitates its extinction for mortalities much smaller than for the 1-prey case.

As an additional effect of the increased number of species and of the variable reduction, we note that data in Figs. 15 and 16 no longer show a sharp predator mortality threshold: it has become blurred. Extinction can occur in a rather wide mortality range, depending of the particular values taken by the rest of parameters.

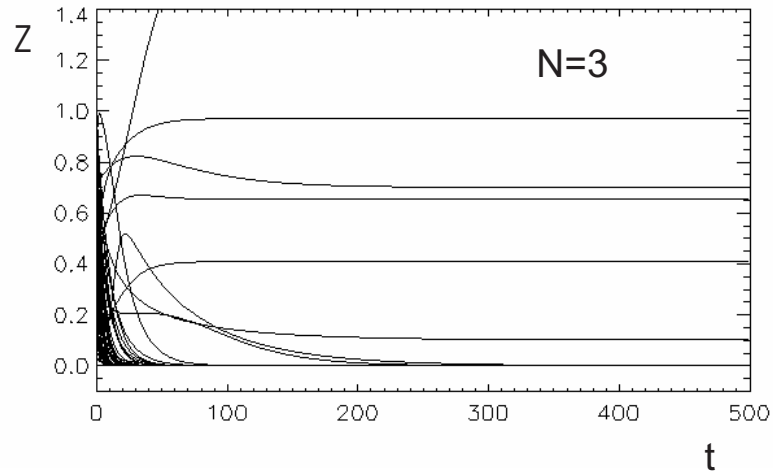


Figure 14: Time evolutions of the consumer (Z) biomass (X) from model (3) with $N = 3$ for several randomly drawn parameter sets.

4 Conclusions

We now summarize our main findings.

- The spatial extension of ecosystems leads unavoidably to the possibility of inhomogeneities. When they are present, observation of a given ecosystem at different scales reveals different patterns. It is a rather general phenomenon that the spatial averaging arising when observation is done at large scales smooths out the system temporal behavior. As an immediate consequence, jumps, bifurcations, and other threshold phenomena may become blurred or even disappear if observed at a too coarse scale. We recover the conclusion in van Nes and Scheffer (2005) stating that large-scale observation of catastrophic regime shifts will be restricted to systems that are relatively homogeneous.
- In addition to smoothing out discontinuities and jumps, the averaging process involved in large-scale descriptions has a more obvious consequence: noise reduction. Noise filtering may have the effect of revealing deterministic patterns that are otherwise hidden inside stochastic fluctuations. The precise outcome of the interplay between these two complementary effects of coarse-graining – blurring of dynamic features and noise clean up – will depend on peculiarities of each system. In the Carpenter et al. (1999) model case shown in Fig. 7, the clearest nonlinear behavior is seen at the smallest

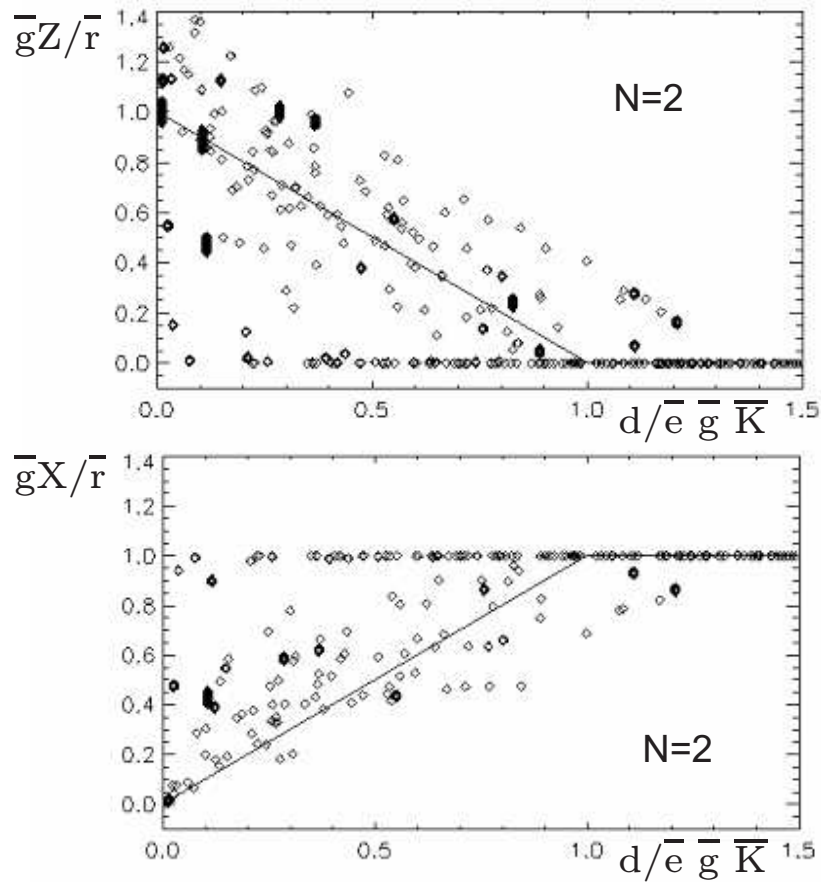


Figure 15: Steady state values of the consumer (Z) biomass and of the aggregated producer biomass (X) from model (3) with $N = 2$ for 500 randomly drawn parameter sets, plotted as a function of the average parameters. Solid line is the analytic result for identical preys.

scales (top plot), whereas in the predator-prey model shown Fig. 2 (Pascual and Levin, 1999) dynamics is better appreciated at intermediate scales (middle plot).

- A different aspect of scale that becomes important in spatially extended ecosystems is system size, and also the precise nature of the conditions affecting the system endpoints. Examples of these effects were shown in Sect. 2.2, together with its interplay with diffusion and noise. It is not easy to extract conclusions valid beyond the scope of the particular model used. One of the observations which seem to be generally valid is the reduction of hysteresis width with increasing noise, in agreement with Guttal

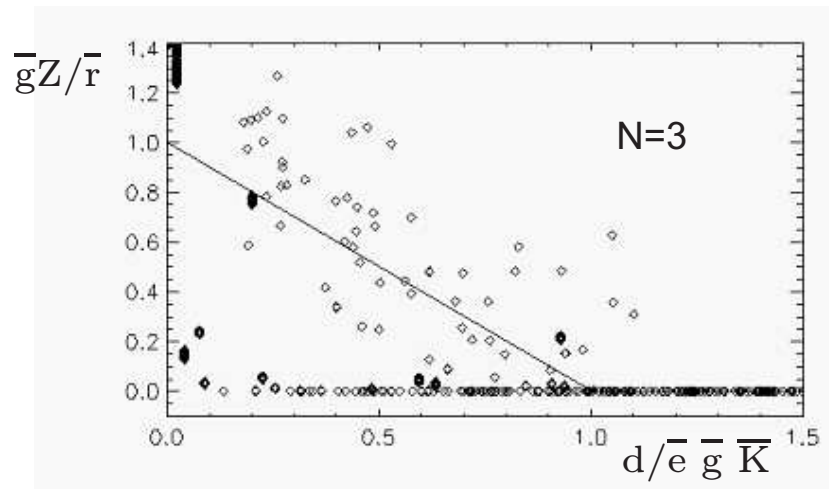


Figure 16: Steady state values of the consumer (Z) biomass from model (3) with $N = 3$ for 500 randomly drawn parameter sets, plotted as a function of the average parameters. Solid line is the analytic result for identical preys.

and Jayaprakash (2006).

- Aggregation of variables into quantities characterizing classes or groups introduces stochasticity in the description, both because fixing the conditions on the coarse variables leaves still undetermined, to a large extent, the finer variables, and because the use of averaged parameter values is usually not enough to fully determine the system fate.
- In the very simple model analyzed in Sect. 3 the impact of this stochasticity is rather strong: the presence of a threshold for consumer extinction becomes blurred and outcomes rather far from what is expected from a reduced description in terms of average parameters occur. The main origin of the strong effects is in the availability of a large number of new solutions when there are more variables, rather than on the modification of particular solutions (which was the case studied in Subsect. 3.1)

The above conclusions summarize the results obtained in the study of aggregation in some particular ecosystem models. Much additional work is needed to find regularities and additional rules that could be of general use when discussing threshold phenomena in ecosystems. Spatial and variable aggregation remain an important topic to consider when modelling and predicting the behavior of complex ecosystems at different scales.

References

- R.A. Armstrong. Grazing limitation and nutrient limitation in marine ecosystems: steady state solutions of an ecosystem model with multiple food chains. *Limn. Ocean.* 39, 597–608 (1994).
- S.R. Carpenter, D. Ludwig, and W.A. Brock. Management of eutrophication for lakes subject to potentially irreversible change. *Ecol. Appl.* 9, 751–771 (1999).
- H. Caswell and M.A. Hohn. From the individual to the population in demographic models. In *Individual-based models and approaches in ecology*, pages 36–61 (Chapman and Hall, New York, 1992).
- X. Chen and J.E. Cohen. Transient dynamics and food-web complexity in the lotka-volterra cascade model. *Proc. R. Soc. Lond. B* 268, 869–877 (2001).
- J.E. Cohen and F. Briand. Trophic links of community food webs. *Proc. Natl. Acad. Sci. USA* 81, 4105–4109. (1984).
- S. de Monte, F. d’Ovidio, H. Chaté, and E. Mosekilde. Noise-induced macroscopic bifurcations in globally coupled chaotic units. *Phys. Rev. Lett.* 92, 254101(1–4) (2004).
- L.E. Gilbert. Food web organization and the conservation of neotropical diversity. In *Conservation of neotropical biology: an evolutionary perspective*, pages 11–33 (Sinauer, Sunderland, MA, 1980).
- T. Gross, W. Ebenhöf, and U. Feudel. Enrichment and food chain stability: the impact of different functional forms. *J. Theor. Biol.* 227, 349–358 (2004).
- V. Guttal and C. Jayaprakash. Impact of noise on bistable ecological systems. *Ecol. Modell., in press* (2006). doi: 10.1016/j.ecolmodel.2006.10.005.
- M.E. Hay. Species as noise in community ecology: do seaweeds block our view of the kelp forest. *Trends Ecol. Evol.* 9, 414–416 (1994).
- E. Hernández-García, C. López, and Z. Neufeld. Spatial patterns in chemically and biologically reacting flows. In *Chaos in Geophysical Flows* (OTTO Editore, Torino, 2003).
- S. Levin. The problem of pattern and scale in ecology. *Ecology* 73, 1943–1967 (1992).

- J. Lundberg and F. Moberg. Mobile link organisms and ecosystem functioning: implications for ecosystem resilience and management. *Ecosystems* 6, 87–98 (2003).
- R.M. May. Will a large complex system be stable? *Nature* 238, 413–414 (1972).
- R.M. May. *Stability and complexity in model ecosystems* (Princeton University Press, Princeton, 1973).
- R. Nathan, G. G. Katul, H. S. Horn, S. M. Thomas, R. Oren, R. Avissar, S. W. Pacala, and S. A. Levin. Mechanisms of long-distance dispersal of seeds by wind. *Nature* 418, 409–413 (2002).
- M. Pascual and H. Caswell. From cell cycle to population cycles in phytoplankton-nutrient interactions. *Ecology* 78, 897–912 (1997).
- M. Pascual and S.A. Levin. From individuals to population densities: searching for the intermediate scale of nontrivial determinism. *Ecology* 80, 2225–2236 (1999).
- M. Pascual, P. Mazzega, and S.A. Levin. Oscillatory dynamics and spatial scale: the role of noise and unresolved pattern. *Ecology* 82, 2357–2369 (2001).
- F. Peters and C. Marrasé. Effects of turbulence on plankton: an overview of experimental evidence and some theoretical considerations. *Mar. Ecol. Prog. Ser.* 205, 291–306 (2000).
- J.P. Sethna. *Statistical Mechanics: Entropy, Order Parameters and Complexity* (Oxford University Press, Oxford, 2006).
- R.S. Steneck and M.N. Dethier. A functional group approach to the structure of algal-dominated communities. *Oikos* 69, 476–498 (1994).
- C.J. Tessone, C.R. Mirasso, R. Toral, and J.D. Gunton. Diversity-induced resonance. *Phys. Rev. Lett.* 97, 194101(1–4) (2006).
- C.J. Tessone, A. Scirè, R. Toral, and P. Colet. Theory of collective firing induced by noise or diversity in excitable media. *Phys. Rev. E* 75, 016203 (1–5) (2007).
- T.F. Thingstad and E. Sakshaug. Control of phytoplankton growth in nutrient recycling ecosystems. theory and terminology. *Mar. Ecol. (Prog. Ser.)* 63, 261–272 (1990).
- E. H. van Nes and M. Scheffer. Implications of spatial heterogeneity for catastrophic regime shifts in ecosystems. *Ecology* 86, 1797–1807 (2005).

G. M. Viswanathan, V. Afanasyev, S. V. Buldyrev, E. J. Murphy, P. A. Prince, and H. E. Stanley. Lévy flight search patterns of wandering albatrosses. *Nature* 381, 413–415 (1996).